Molecular Immunology 101 (2018) 55–64

Contents lists available at ScienceDirect

Molecular Immunology

journal homepage: www.elsevier.com/locate/molimm

The influence of TAP1 and TAP2 gene polymorphisms on TAP function and its inhibition by viral immune evasion proteins

P. Praest[1], R.D. Luteijn[1,2], I.G.J. Brak-Boer, J. Lanfermeijer, H. Hoelen, L. Ijgosse, A.I. Costa, R.D. Gorham Jr., R.J. Lebbink, E.J.H.J. Wiertz*

Department of Medical Microbiology, University Medical Center Utrecht, 3584CX Utrecht, The Netherlands

ARTICLE INFO

Keywords:
TAP
Polymorphism
Antigen presentation
Viral immune evasion
Herpesviruses

ABSTRACT

Herpesviruses encode numerous immune evasion molecules that interfere with the immune system, particularly with certain stages in the MHC class I antigen presentation pathway. In this pathway, the transporter associated with antigen processing (TAP) is a frequent target of viral immune evasion strategies. This ER-resident transporter is composed of the proteins TAP1 and TAP2, and plays a crucial role in the loading of viral peptides onto MHC class I molecules. Several variants of TAP1 and TAP2 occur in the human population, some of which are linked to autoimmune disorders and susceptibility to infections. Here, we assessed the influence of naturally occurring TAP variants on peptide transport and MHC class I expression. In addition, we tested the inhibitory capacity of three viral immune evasion proteins, the TAP inhibitors US6 from human cytomegalovirus, ICP47 from herpes simplex virus type 1 and BNLF2a from Epstein-Barr virus, for a series of TAP1 and TAP2 variants. Our results suggest that these TAP polymorphisms have no or limited effect on peptide transport or MHC class I expression. Furthermore, our study indicates that the herpesvirus-encoded TAP inhibitors target a broad spectrum of TAP variants; inhibition of TAP is not affected by the naturally occurring polymorphisms of TAP tested in this study. Our findings suggest that the long-term coevolution of herpesviruses and their host did not result in selection of inhibitor-resistant TAP variants in the human population.

1. Introduction

The immune system recognizes altered cells through changes in the peptide repertoire presented by major histocompatibility complex class I (MHC I) molecules. MHC I molecules at the surface of infected cells present antigenic peptides to cytotoxic $CD8^+$ T-cells (CTLs). These adaptive immune cells mount an immune response upon recognition of an antigenic peptide by their T-cell receptor.

The majority of peptides presented by MHC I are generated by constant turnover of proteins by the cytosolic proteasome. The resulting peptides are transported into the endoplasmic reticulum (ER) by the transporter associated with antigen processing (TAP). In the ER, TAP and other proteins of the MHC class I peptide-loading complex (PLC) promote folding of MHC I molecules and ensure proper loading of peptides into the MHC I peptide binding groove (Sadasivan et al., 1996). Upon stable peptide loading, the peptide-MHC I complex is translocated to the cell surface, where it displays the peptides to $CD8^+$ CTLs.

TAP plays a central role in MHC I antigen presentation, as illustrated by the reduced surface expression of MHC I in cells lacking (functional) TAP. In these cells, empty MHC I molecules are retained in the ER lumen and consequently are unable to display antigens to the immune system (Ljunggren et al., 1990; Townsend et al., 1989). Due to its crucial role in MHC I antigen presentation, TAP has become an attractive target for viral immune evasion strategies. During a long period of virus-host coevolution, herpesviruses independently acquired highly efficient ways to block TAP-mediated peptide transport (Verweij et al., 2015). The viral TAP-inhibitors identified so far have no structural homology and bind to distinctive domains of the transporter (van de Weijer et al., 2015).

The TAP heterodimer is composed of TAP1 (ABCB2) and TAP2 (ABCB3), members of the ATP-binding cassette (ABC) family (Dean and Annilo, 2005). TAP1 and TAP2 both consist of a nucleotide-binding domain (NBD) and multiple transmembrane domains (TMDs). The core of the TAP heterodimer is comprised of 12 transmembrane domains (six from each TAP subunit), and the cytosolic NBDs. TAP1 and TAP2 have

* Corresponding author.
E-mail address: e.wiertz@umcutrecht.nl (E.J.H.J. Wiertz).
[1] These authors contributed equally to this study.
[2] Current address: Department of Molecular and Cell Biology, University of California, Berkeley, CA 94706, United States.

https://doi.org/10.1016/j.molimm.2018.05.025
Received 19 February 2018; Received in revised form 23 May 2018; Accepted 28 May 2018
Available online 04 June 2018

additional transmembrane helices (TMD0 domains) at their N-termini (four in TAP1, three in TAP2), which flank the core region (Koch et al., 2004). The core domains of TAP are necessary and sufficient to allow for peptide translocation from the cytosol to the ER to occur. This process requires ATP binding and hydrolysis (Neefjes et al., 1993), whereas peptide binding to TAP itself is ATP-independent (van Endert et al., 1994). TAP contains several domains that are highly conserved throughout the ABC transporter family. These regions are mainly located at the C-terminal NBDs that include the Walker A and B motifs for ATP binding and hydrolysis, the switch domain, and the C-motif (Gaudet and Wiley, 2001; McCluskey et al., 2004; Walker et al., 1982).

Sequence analysis has revealed that for the human TAP (hTAP) 1 and 2 genes several single nucleotide polymorphisms (SNPs) have been maintained within the population. These SNPs are dispersed throughout the TAP-encoding genes, including regions highly conserved between ABC transporters (McCluskey et al., 2004). Several of these SNPs are more prevalent among certain ethnical groups, whereas others are more equally distributed in the human population (Lajoie et al., 2003; Tang et al., 2001a,b). In addition, a number of these TAP SNPs have been linked to the susceptibility to or severity of several diseases, including tuberculosis(Naderi et al., 2016; Wang et al., 2012), Alzheimer's disease (Bullido et al., 2007), alopecia areata (Kim et al., 2015), hematological malignancies (Ozbas-Gerceker et al., 2013), and cervical intraepithelial neoplasia (Natter et al., 2013). Mutational analysis of the rat TAP2 gene revealed that SNPs can result in severe changes in substrate selectivity (Powis et al., 1996). In contrast, the few hTAP allelic variants tested thus far did not impact substrate specificity and TAP activity as compared to the most common TAP variants (Daniel et al., 1997; Obst et al., 1995). Therefore, it remains unknown why TAP variants are maintained within the population, and if such polymorphisms have evolved under selective pressure. Evolutionary pressure by viruses, and in particular herpes viruses, has likely driven polymorphism in other components of the immune system, including MHC I (Borghans et al., 2004; Carrillo-Bustamante et al., 2015; Kubinak et al., 2013; Potts and Slev, 1995). Similarly, evolutionary pressure by viral TAP inhibitors may have shaped the SNPs in the TAP-encoding genes, thereby disarming these viral inhibitors.

In this study, we evaluated the influence of TAP polymorphisms on peptide transport. In addition, inhibition of a series of TAP variants by TAP inhibitors encoded by three common human herpesviruses, human cytomegalovirus (HCMV), herpes simplex virus type 1 (HSV-1) and Epstein-Barr virus (EBV), was investigated.

2. Materials and methods

2.1. Cell culture

The human melanoma cell line MelJuSo (MJS) was cultured in RPMI 1640 (Invitrogen) containing 10% FCS (PAA laboratories), 100 U/ml penicillin, 100 µg/ml streptomycin and 2 mM L-glutamine (complete RPMI medium). HEK293T cells used for lentivirus production were cultivated and maintained in DMEM (Invitrogen) supplemented with 10% FCS (PAA laboratories), 100 U/ml penicillin, 100 µg/ml streptomycin and 2 mM L-glutamine (complete DMEM medium).

2.2. Plasmids

A selectable CRISPR/Cas9 vector based on the pSicoR vector (Addgene plasmid 11579, Tyler Jacks Lab, MIT) was constructed as described previously (van de Weijer et al., 2014; van Diemen et al., 2016). This lentiviral vector includes a human codon-optimized *S. pyogenes* Cas9 gene N-terminally fused to a puromycin resistance gene *via* a T2A ribosome-skipping sequence under control of the human EF1A promoter. In addition, this vector has a human U6 promoter that induces expression of a guideRNA (gRNA) consisting of a 20 bp target-specific CRISPR RNA (crRNA) fused to the *trans*-activating crRNA (tracrRNA) and a terminator sequence. This vector is called pSicoR-CRISPR-PuroR.

Table 1
TAP1 alleles used in this study.

Allele	Mutations present in allele
TAP1*01:01	Reference
TAP1*01:01-long	alternative start site at position -60 used
TAP1*02:01	I333V, D637G
TAP1*03:01	I333V
TAP1*01:04	I333V, V458L. D637G, R648Q
TAP1*x	I333V, A370V, V518I, D637G
TAP1-G17R	G17R
TAP1-G247R	G247R
TAP1-S286F	S286F
TAP1-Q728K	Q728K

For TAP1 overexpression and rescue experiments, a dual promoter lentiviral plasmid expressing puroR and GFP under control of the human PGK promoter was used (pPuroR-GFP; PMID 24807418). TAP1 variants (see Table 1) were introduced downstream of the human EF1a promoter using Gibson assembly (#E2611L, Bioké, New England Biolabs). For TAP2 overexpression and rescue experiments, TAP2 variants were introduced into a dual promoter lentiviral vector expressing the Zeocin resistance gene and mAmetrine (pZeoR-mAmetrine).

For overexpression of the viral TAP inhibitors, a dual promoter lentiviral vector expressing a blasticidin resistance gene (pBlastR) was used. Genes encoding viral TAP inhibitors were introduced downstream of an EF1a promoter using Gibson assembly.

2.3. Generation of MJS cells with TAP1 and TAP2 double KO

To generate MJS cells lacking TAP2, cells were transfected with pSico-CRISPR-PuroR containing the TAP2-targeting crRNA sequence 5'-GGAAGAAGAAGGCGGCAACG-3'. After transfection and selection with puromycin (2 µg/ml), cells were cloned by limiting dilution. To prove the absence of TAP2, individual clones were analyzed by (i) immunoblotting (IB), (ii) sequencing of the genomic target site, and (iii) flow cytometry to evaluate cell surface expression of MHC I. A clone lacking TAP2 was subsequently transfected with a pSicoR-CRISPR-PuroR vector containing the TAP1-targeting crRNA sequence 5'-GGGG TCCTCAGGGCAACGGT-3'. After transfection and selection with puromycin, cells were cloned by limited dilution and TAP1 expression was analyzed by IB. Genomic DNA sequence analysis of the TAP2 gRNA target site revealed a deletion of an A nucleotide and a substitution of a C for a T nucleotide in one allele, and an insertion of an A nucleotide in the other allele. Both mutations induce a frameshift in the reading frame of the TAP2 gene. Genomic DNA sequence analysis of the TAP1 gRNA target site revealed a 31bp deletion. No other mutated or wt sequences were uncovered. A monoclonal cell line lacking TAP1 and TAP2 was used for further experiments.

2.4. Generation of TAP alleles

The TAP1-encoding gene was C-terminally tagged with a streptavidinII-tag using primers 1 and 47. The TAP2-encoding gene was C-terminally tagged with a His-tag using primers 15 and 48. To generate the different TAP variants, the vectors encoding the reference sequences TAP1*01:01-Strep and TAP2*01:01-His were used as templates for PCR amplification. The TAP1*01:01 reference allele with the canonical translation start site was generated using primers 1 and 2. The template for these primers was a vector that encodes the TAP*01:01-long allele. This allele encodes a 5'-extended TAP1*01:01 variant that uses an alternative in frame start site 60bp upstream of the canonical translation start site. This long variant was generated using gBLOCKs (Integrated DNA Technologies). The TAP1*01:01 reference

allele was then used to generate the remaining TAP1 alleles. Primers 3–6 for TAP1*02:01, primers 3–4 for TAP1*03:01, primers 3–6 and 33–36 for TAP1*01:04, primers 3–6 and 37–40 for TAP1*x, primers 7–8 for TAP1-G17R, primers 9–10 for TAP1-G247R, primers 11–12 for TAP1-S286F and primers 13–14 for TAP1-Q728K were used. For the generation of the TAP2 alleles, primers 15–16 for TAP2*01:02, primers 17–18 for TAP2*01:03, primers 19–22 for TAP2*02-01, primers 19–26 for TAP2*02D, primers 17, 18, 23, 24, 25 and 26 for TAP2*1G, primers 15,16 and 19–24 for TAP2*2F, primers 21–22 and 29–30 for TAP2*BKY and primers 31 and 32 for TAP2-A513S were used (Supplementary Table S1).

2.5. Generation of viral inhibitor-constructs

Viral inhibitors were myc-tagged by PCR. The myc tag was added to the C-terminus of US6 (Hewitt et al., 2001) (using primers 41 and 42, see Supplementary Table S2) and BNLF2a (Horst et al., 2009) (using primers 43 and 44) and to the N-terminus of ICP47 (Ahn et al., 1996) (using primers 45 and 46).

2.6. Lentivirus production and transduction

For the production of replication-deficient recombinant lentiviruses, the lentiviral vectors and third-generation packaging vectors pVSV-G, pMDL and pRSV were co-transfected into HEK293T cells using PEI (1 mg/ml). Lentivirus-containing supernatants were harvested after 3 days and used to transduce MJS cells by spin infection at 2000 rpm for 90 min at 33 °C in the presence of 4 μg/ml polybrene (Santa Cruz Biotechnology). Selection media containing puromycin (2 μg/ml), blasticidin (20 μg/ml) and zeocin (400 μg/ml) were applied 3 days post infection.

2.7. Immunoblotting (IB)

Cells were harvested and washed with ice-cold PBS, and lysed in 1% Triton X-100 (PanReac) lysis buffer supplemented with 150 mM NaCl and 50 mM Tris-HCl pH 8 for 30 min on ice. The cell lysates were centrifuged at 22,000 *g* for 15 min at 4 °C to remove cellular debris. The supernatants were mixed with Laemmli sample buffer supplemented with 80 mM DTT (Sigma) and loaded on 12% NuPage or 4–12% BOLT SDS gels (Thermo Scientific). The proteins were transferred to Trans-Blot Turbo PVDF membranes (BIO-RAD) using a Trans-Blot Turbo transfer system (BIO-RAD) for 10 min at 25 V or using the Mini Trans-Blot Cell system (BIO-RAD) overnight at a constant 12 V at 4 °C. The membranes were blocked with 4% milk powder (Campina) in phosphate-buffered saline supplemented with 0.05% Tween 20 (PBST) for 1 h at 4 °C. Primary antibodies were diluted in PBST and incubated with the membranes overnight at 4 °C. The membranes were washed thoroughly with PBST at 4 °C and were then incubated with a labelled secondary antibody for 2 h at 4 °C. Membranes were again washed thoroughly at 4 °C. Chemiluminescence was detected using Pierce ECL Western Blotting Substrate (Thermo Scientific), followed by exposure of the membranes to Amersham Hyperfilm ECL films (GE Healthcare).

2.8. MHC I surface expression

MHC-I surface expression was assessed by flow cytometry using a FACS Canto II (BD Biosciences). Cells were washed with PBS and stained for 30 min with a PE-conjugated antibody (W6/32) at the concentrations indicated in cold PBS supplemented with 0.5% BSA and 0.02% NaN_3 in a total volume of 20 μl. The cells were washed to remove unbound antibody and then fixed in PBS supplemented with 1% formaldehyde, 0.5% BSA and 0.02% NaN_3. The data were analyzed using FlowJo V10 software.

2.9. Peptide translocation assay

The peptide translocation assay was performed as described previously (Fischbach et al., 2015). Briefly, cells were permeabilized using 2.9 mg/ml of Streptolysin-O (SLO, Murex Diagnostics) at 4 °C for 15 min, and washed with PBS supplemented with 10 mM $MgCl_2$ to remove residual SLO. Permeabilized cells were incubated with 20 nM of a synthetic peptide carrying a fluorescein moiety; the following peptides have been used: (FL)-V-N-K-T-E-R-A-Y (used for all transport assays described in this study) and R-R-Y-Q-N-S-T-C-(FL)-L (used in Supplementary Fig. 1 only). The peptides have been kindly provided by Dr. Jan Wouter Drijfhout, Department of Immunohematology and Blood Transfusion, Leiden University Medical Center, Leiden, The Netherlands. Incubation was performed in the presence of 10 mM ATP or 20 mM ADP supplemented with 10 mM $MgCl_2$ for 15 min at 37 °C in a total volume of 50 μl. Transport was terminated by adding 150 μl PBS supplemented with 20 mM EDTA. The stained cells were analyzed by flow cytometry with a FACS Canto II (BD Biosciences).

2.10. Antibodies

The following primary and secondary antibodies were used for IB: mouse-anti-human TAP1 148.3 C-terminus mAb (1:200) (Plewnia et al., 2007), mouse-anti-human TAP2 435.4 mAb (1:200) (van Endert et al., 1994), mouse-anti-myc 9E10 mAb (1:1000), mouse-anti-actin mAb (Millipore MAB1501R, 1:10,000), mouse-anti-transferrin receptor mAb (Santa Cruz sc-7327, 1:1000), goat-anti-mouse conjugate-HRP pAb (Jackson #115-035-174, 1:5000) and goat-anti-rat-HRP (Jackson #112-035-175,1:5000). For flow cytometry, the following antibodies were used: PE-conjugated W6/32, anti-HLA-I (Serotec MCA81PE, 1:20).

2.11. Molecular modeling

The molecular structures of the TAP1-TAP2 and TAP1-TAP2-ICP47 complexes were generated using the atomic model based on the high-resolution cryo-EM structure of the TAP1-TAP2-ICP47 complex (PDB code 5U1D) (Oldham et al., 2016a). Missing loops and termini within each molecule were built using Modeller (Webb et al., 2014). TAP1 and TAP2 molecules were renumbered according to the numbering scheme in Uniprot entries Q03518 and Q03519, respectively, in order to locate and display all residues affected by SNPs. All SNPs were depicted with the exception of the TAP1 SNP G17R, as it occurs in the N-terminal TMD of TAP1 that was not resolved in the original cryo-EM structure. All figures were rendered using Chimera (Pettersen et al., 2004).

3. Results

3.1. Mapping of SNPs in TAP1 and TAP2

In this study, the most common TAP alleles in the human population were investigated (Tables 1 and 2) (Powis et al., 1993), as well as a number of less frequent alleles with non-synonymous polymorphisms

Table 2
TAP2 alleles used in this study.

Allele	Mutations present in allele
TAP2*01:01	Reference
TAP2*01:02	A565S
TAP2*01:03	R651C
TAP2*02:01	T665A, STOP687Q
TAP2*2D	A374T, V467I, T665A, STOP687Q
TAP2*1G	A374T, V379I, R651C
TAP2*2F	V379I, A565S, T665A, STOP687Q
TAP2*BKY	M577V, STOP687Q
TAP2-A513S	A513S

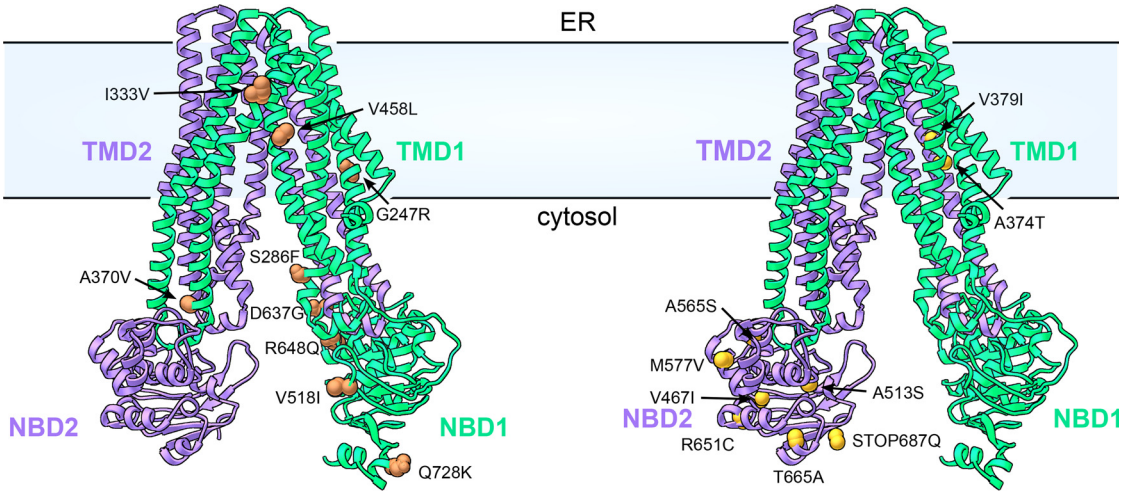

Fig. 1. Molecular model of the heterodimeric human TAP complex including SNP's of TAP1 and TAP2. The structure of TAP1 including its cytosolic nucleotide binding domain (NBD1) and its six transmembrane regions forming the core transmembrane domain (TMD1) is depicted in green. The structure of the NBD2 and TMD2 of TAP2 is shown in purple. Non-synonymous SNPs in TAP1 evaluated in this study are shown in orange (left). G17R is not shown because it occurs in the N-terminal TMD not present in the model. The TAP2 SNPs included in this study are shown in yellow (right). (For interpretation of the references to colour in this figure legend, the reader is referred to the web version of this article.)

that might affect TAP function. The alleles studied include variants that change the biochemical properties of the amino acid side chains, as well as alleles that carry polymorphisms in highly conserved regions. To highlight the location of these variations within the TAP heterodimer, a molecular model of TAP is displayed in Fig. 1. Three out of the ten TAP1 SNPs are located in the NBD of TAP1, whereas seven out of the nine TAP2 SNPs are located in the NBD of TAP2. The SNPs A374T and V379I are positioned in the TMD of TAP2.

3.2. Generation of a monoclonal TAP1 and TAP2 KO cell line

To investigate the effect of variations within TAP1 and TAP2 on peptide transport and MHC I surface expression, MJS cells lacking TAP1 and TAP2 were generated. As TAP2 is unstable in the absence of TAP1 (Keusekotten et al., 2006), TAP1/TAP2 double knock-out cells were generated by sequential deletion of TAP2 and TAP1 using the CRISPR/Cas9 technology. The lack of TAP1 and TAP2 expression was confirmed by immunoblotting (Fig. 2A) and sequencing of the TAP alleles (data not shown). As expected, TAP1/TAP2 double KO cells had severely reduced MHC I surface expression levels as compared to MJS WT cells (Fig. 2B, green *vs.* blue). MHC I surface expression was restored upon reintroduction of TAP1 and TAP2 (red; shown for the reference genes TAP1*01:01 and TAP2*01:01).

3.3. The effect of TAP1 and TAP2 polymorphisms on TAP function

The TAP variants (Table 1) were expressed in TAP1/TAP2 KO cells as combinations of the TAP1 reference allele and TAP2 variants, or *vice versa*. Expression of all TAP1 and TAP2 variants was verified by immunoblotting using antibodies specific for TAP1 or TAP2 (Fig. 3A and B, respectively). Most variants were expressed at similar levels; TAP1*01-04, TAP1*G247R and TAP2*1G were consistently present at slightly higher levels (Fig. 3A).

To assess TAP function, a peptide transport assay was used. Peptide translocation from the cytosol into the ER was measured using a fluorescein-labelled peptide, (FL)-V-N-K-T-E-R-A-Y, in the presence of ATP (active transport) or ADP (passive diffusion). The transport activity of the variants and controls was normalized to the levels observed in wild type cells. In the presence of ATP, peptide transport by the TAP1 and TAP2 variants showed some variation, yet it was mostly similar to the transport activity of wild-type cells. Upon addition of ADP, almost no transport was observed in wild type cells (Fig. 3C and D) or cells

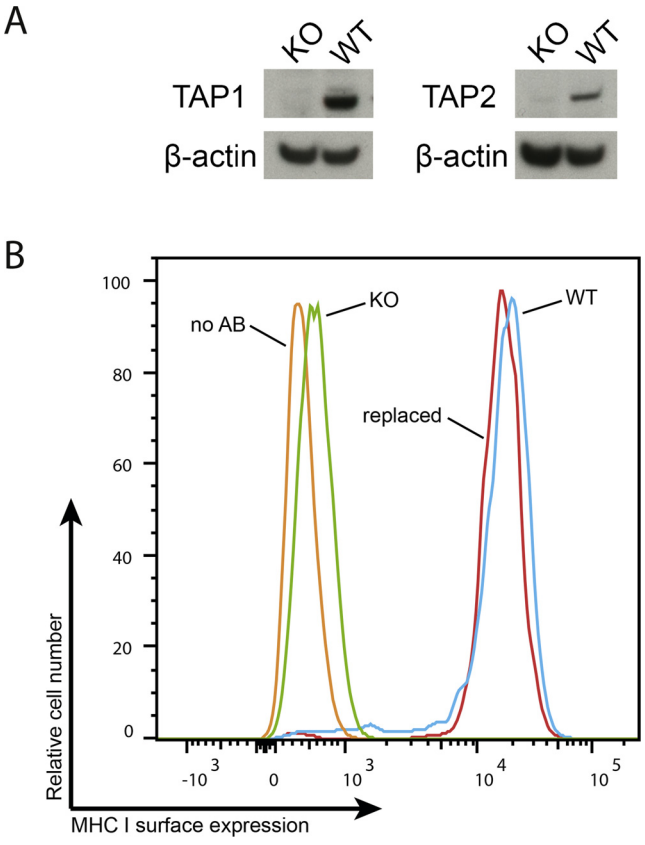

Fig. 2. Confirmation of the knock-out phenotype of TAP1/2 KO MJS cells. (A) Lysates from MJS WT cells and TAP1/2 KO MJS cells stained for TAP1 and TAP2 by immunoblotting (IB) with specific antibodies. β-actin was used as a loading control. (B) Surface expression of MHC I molecules of TAP1/2 KO MJS cells (green), TAP1/2 KO MJS cells reconstituted with TAP1/2 (red), MJS WT cells (blue) and unstained MJS WT cells (orange) was assessed by flow cytometry. (For interpretation of the references to colour in this figure legend, the reader is referred to the web version of this article.)

expressing TAP variants (data not shown). The level of peptide transport in the presence of ADP was similar to that in TAP1 and TAP2 KO cells. Similar levels of peptide transport were observed when using a

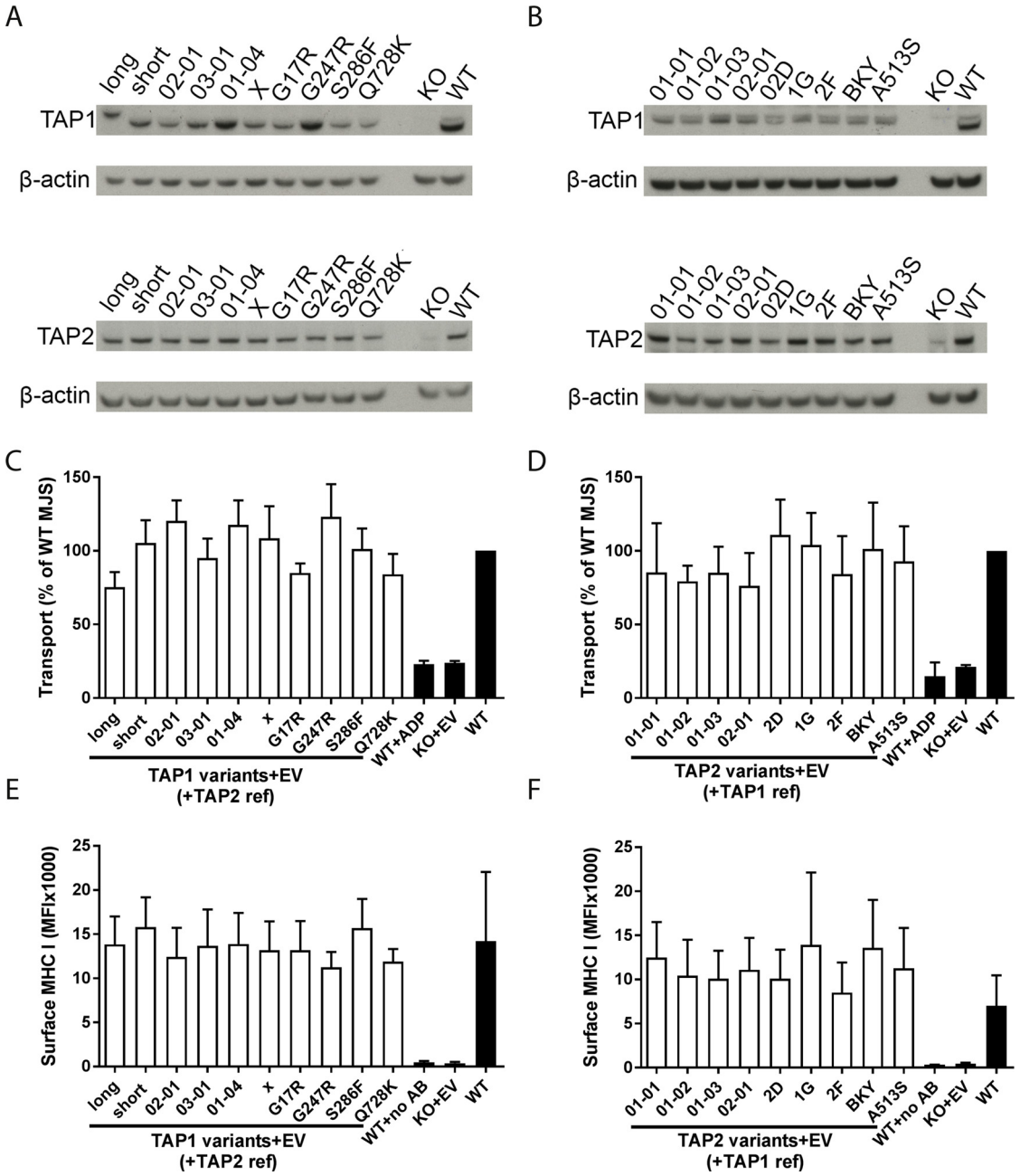

Fig. 3. Expression and function of TAP1 and TAP2 variants introduced into TAP1/2 KO MJS cells. Expression of TAP1 variant-TAP2 reference pairs (A) and TAP2 variant-TAP1 reference pairs (B) in MJS cells was analyzed by immunoblotting (IB) of lysates with specific antibodies. TAP expression was compared to that of TAP WT cells; lysates of TAP KO cells served as negative control. β-actin was used as a loading control. (C and D) TAP-dependent peptide translocation in MJS cells transduced with the different variant-reference pairs, displayed as changes in mean fluorescence intensity (MFI), normalized to that of MJS WT cells. MJS WT cells incubated with ADP were used to verify that transport is ATP dependent. TAP1/2 KO cells transduced with an empty vector (EV) were used as a control. (E and F) Relative surface expression levels of MHC I molecules on MJS containing the different TAP variants compared to MJS WT, assessed by flow cytometry. MJS without antibody and TAP1/2 KO MJS were included as controls. Error bars indicate the SD, N = 3.

different fluorescent peptide, R-R-Y-Q-N-S-T-C-(FL)-L (Supplementary Fig. 1). As the results were similar, subsequent experiments were performed with the peptide (FL)-V-N-K-T-E-R-A-Y.

Next, we assessed the relative MHC I surface expression levels in the presence of the various TAP variants as compared to wild type cells and TAP1/2 KO cells (Fig. 3E and F). The TAP variants showed some variation of MHC I surface expression, but the levels did not differ drastically from those observed in wild type cells.

3.4. Inhibition of peptide transport and MHC I surface expression by viral TAP inhibitors in cells expressing TAP1 and TAP2 variants

Next, we tested the ability of these TAP variants to escape inhibition by the TAP inhibitors US6 from HCMV, ICP47 from HSV-1 and BNLF2a from EBV. These viral proteins may affect the TAP variants differently, thereby providing a rationale for the existence of TAP polymorphisms in the human population. The viral inhibitors and the various TAP alleles were introduced in the TAP1/TAP2 KO cells through lentiviral transduction. Peptide transport was evaluated in the resulting cell lines using a functional assay; in addition, MHC I surface expression was

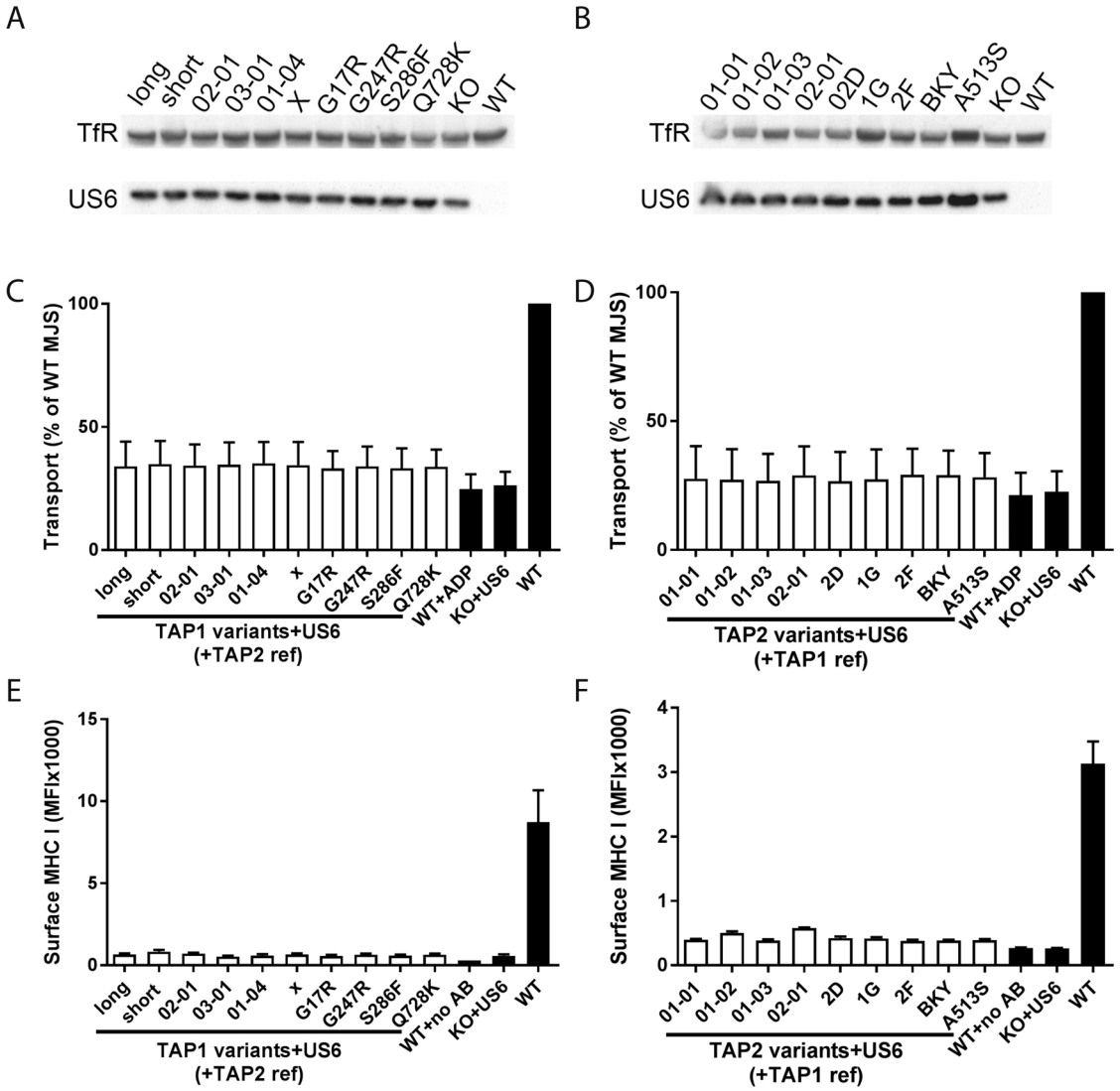

Fig. 4. Inhibition of TAP function by the viral inhibitor US6. Expression of US6 in MJS containing the TAP1 variant-TAP2 reference pairs (A) and TAP2 variant-TAP1 reference pairs (B) was analyzed by immunoblotting (IB) of lysates with a mouse-anti-myc antibody. Lysates of TAP KO and untransduced WT cells served as controls. TfR was used as a loading control. (C and D) TAP-dependent peptide translocation in MJS cells transduced with the viral inhibitor US6 and different variant-reference pairs, displayed as changes in MFI, normalized to that of MJS WT cells. MJS WT cells incubated with ADP were used to verify that transport is ATP dependent. TAP1/2 KO cells transduced with the inhibitor US6 were used as a control. (E and F) Relative surface expression levels of MHC I molecules on MJS containing the different TAP variants and US6 compared to MJS WT cells, assessed by flow cytometry. MJS without antibody and TAP1/2 KO MJS cells + US6 were used as controls. Error bars indicate the SD, N = 3.

quantified (Fig. 4–6).

The presence of the myc-tagged viral inhibitor US6 was confirmed by immunoblotting using a myc tag-specific antibody. The cells showed similar expression levels of US6 (Fig. 4A and B). The peptide translocation activity was normalized to the activity of MJS wild type cells (Fig. 4C and D). In the presence of US6, peptide translocation *via* the TAP variants was strongly inhibited, to levels similar to those in the presence of ADP, or in the absence of TAP1 and TAP2. In addition, the TAP variants tested did not differ in translocation activity.

Next, MHC I surface levels were assessed in the presence of US6. The reduction of MHC I surface expression confirmed the inhibition of TAP by the viral US6 protein (Fig. 4E and F). All TAP1 and TAP2 variants showed an equally strong reduction of cell surface MHC I levels that was comparable to cells containing the viral inhibitor yet lacking TAP1 and TAP2.

Next, the inhibitory effect of the viral inhibitors BNLF2a and ICP47 on the TAP1/TAP2 variants was analyzed. The presence of the inhibitors was confirmed by immunoblotting for BNLF2a (Fig. 5A and B), and by sequencing for ICP47 (data not shown; no antibody with sufficient sensitivity is available for immunoblotting of ICP47). BNLF2a and ICP47 were found to inhibit all TAP variants equally well, reducing peptide transport levels to those observed in TAP1 and TAP2 KO cells (Fig. 5C,D and Fig. 6A,B, respectively). In agreement with this, MHC I surface expression was reduced to background levels in the presence of both inhibitors (Fig. 5E,F and Fig. 6C,D, respectively).

In conclusion, all TAP1 and TAP2 variants were inhibited to a similar extent by the three herpesvirus-encoded TAP inhibitors.

4. Discussion

In this study, we addressed the functional consequences of TAP1 and TAP2 SNPs for peptide transport activity. In addition, we evaluated whether these SNPs influence inhibition of TAP by viral TAP inhibitors. Our results suggest that the SNPs present in a diverse collection of TAP variants have little or no effect on the peptide transport activity of the complex. Furthermore, the different TAP SNPs did not influence the

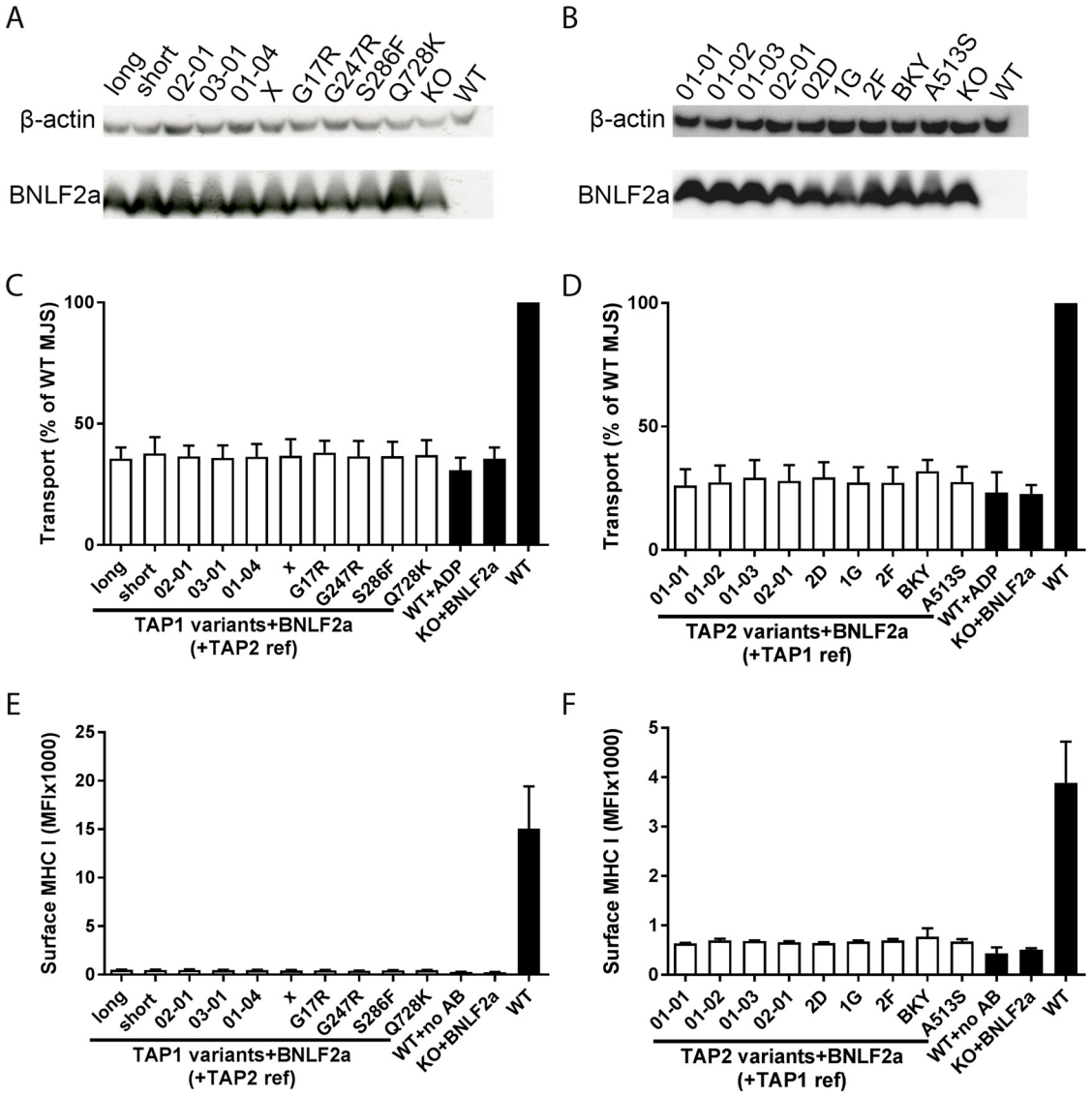

Fig. 5. Inhibition of TAP function by the viral inhibitor BNLF2a. Expression of BNLF2a in MJS cells containing the TAP1 variant-TAP2 reference pairs (A) and TAP2 variant-TAP1 reference pairs (B) was analyzed by immunoblotting (IB) of lysates with a mouse-anti-myc antibody. Lysates of TAP KO cells served as negative control. β-actin was used as a loading control. (C and D) TAP-dependent peptide translocation in MJS cells transduced with the viral inhibitor BNLF2a and different variant-reference pairs, displayed as changes in MFI, normalized to that of MJS WT cells. MJS WT cells incubated with ADP were used to verify that transport is ATP dependent. TAP1/2 KO cells transduced with the inhibitor BNLF2a were used as a control. (E and F) Relative surface expression levels of MHC I molecules on MJS containing the different TAP variants and BNLF2a compared to MJS WT cells, assessed by flow cytometry. MJS without antibody and TAP1/2 KO MJS cells + BNLF2a were used as controls. Error bars indicate the SD, N = 3.

inhibitory capacity of the viral immune evasion proteins ICP47, US6 and BNLF2a.

For some of the variants, expression was consistently higher compared to the other variants tested, for example for TAP1*01:04, TAP1*G247R and TAP2*1G. Possibly, certain SNPs influence the stability of TAP. However, higher or lower expression levels do not seem to correlate directly with increased or decreased transport activity. Over all, variation in TAP1 and TAP2 protein expression did not correlate with TAP activity *in vitro*.

Our findings are in agreement with a previous study comparing the peptide transport capacity of the TAP1 alleles 01-01, 02-01, and 03-01, and the TAP2 alleles 01-01, 02-01, and 01-02 (Daniel et al., 1997; Obst et al., 1995). No major differences in TAP transport activity or MHC I surface levels were observed for these TAP alleles.

Several polymorphisms are located in, or in close proximity to, highly conserved regions known to be important for TAP function (McCluskey et al., 2004). The polymorphism D637 G present in the TAP alleles TAP1*02:01, TAP1*01:04 and TAP1*x results in a change in biochemical properties, as a negatively charged aspartic acid is replaced by a non-polar uncharged glycine. This polymorphism is in close proximity to the C-loop and Walker B domain. Both regions play a role in the binding and hydrolysis of ATP (Parcej and Tampé, 2010). Nevertheless, the transport activity of the variants carrying this SNP was not very different from that measured in WT cells. The TAP alleles TAP1*02:01,TAP1*01:04 and TAP1*x, as well as TAP1*03:01 contain the SNP I333V. The polymorphism I333V is associated with a higher risk of cervical intraepithelial neoplasia after infection of HPV (Natter et al., 2013). In the present study, the TAP1*03:01 allele did not exhibit dramatic changes in MHC I surface expression nor did it affect peptide translocation in absence or presence of the viral inhibitors in comparison to the other alleles and the WT cells. It remains possible that peptides highly specific for certain diseases are better transported by certain TAP variants. This may not be reflected by assays measuring overall transport activity or MHC I surface expression.

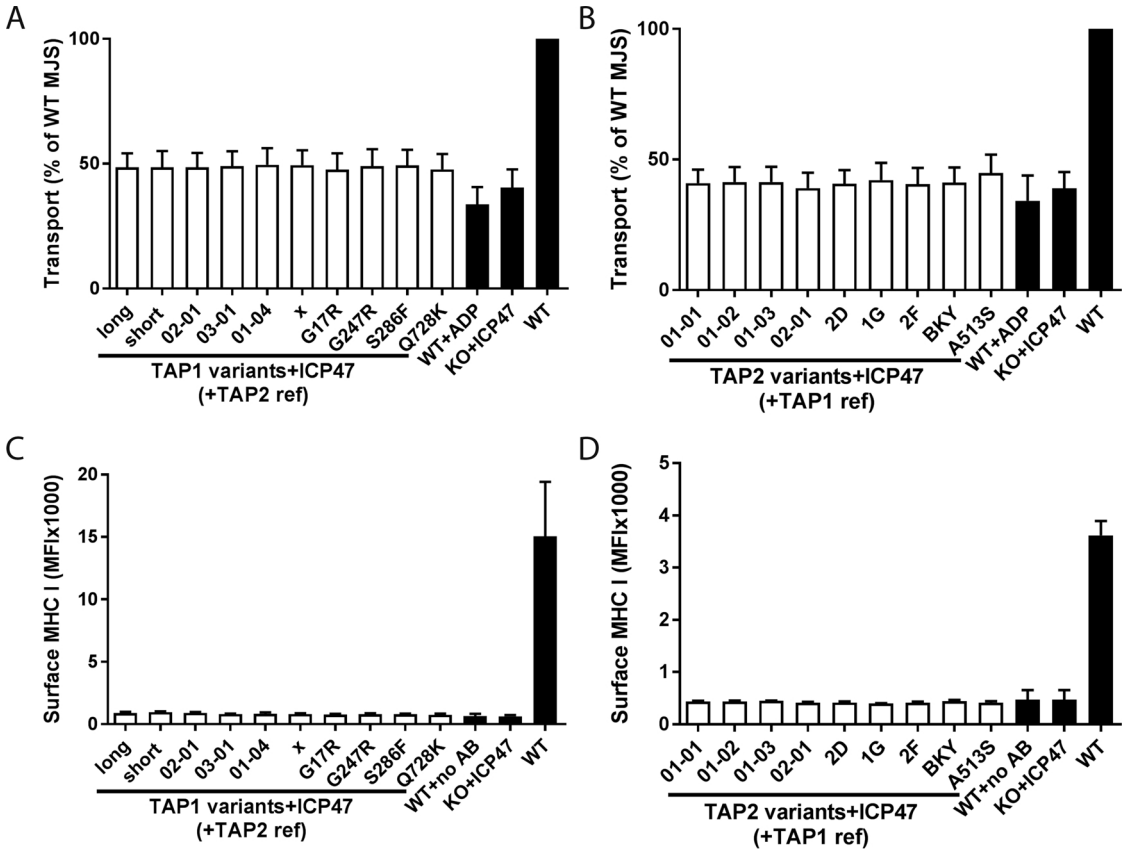

Fig. 6. Inhibition of TAP function by the viral inhibitor ICP47. (A and B) TAP-dependent peptide translocation in MJS cells transduced with the viral inhibitor ICP47 and different variant-reference pairs, displayed as changes in MFI, normalized to that of MJS WT cells. MJS WT cells incubated with ADP were used to verify that transport is ATP dependent. TAP1/2 KO cells transduced with the inhibitor ICP47 were used as a control. (C and D) Relative surface expression levels of MHC I molecules on MJS containing the different TAP variants and ICP47 compared to MJS WT cells, assessed by flow cytometry. MJS without antibody and TAP1/2 KO MJS cells + ICP47 were used as controls. Error bars indicate the SD, N = 3.

Regions comprising residues 375–420 and 453–487 of TAP1 and residues 301–389 and 414–433 of TAP2 form part of the peptide binding site (Nijenhuis and Hämmerling, 1996). Interestingly, several TAP variants have SNPs in or in close proximity to the peptide binding site, including TAP1 SNPs I333V, A370V and S286F and TAP2 SNPs A374T and V379I. However, the transport activity of TAP proteins containing these polymorphisms is within the same range.

Certain TAP alleles show differences in frequency amongst Africans, Caucasians and Brazilians (Tang et al., 2001b). These polymorphisms may have emerged within populations due to evolutionary pressure exerted by certain pathogens occurring in these geographically distinct regions (Lajoie et al., 2003). US6, BNLF2a and ICP47 block different TAP-variants equally well and are therefore unlikely to have caused selection pressure on the different SNPs of TAP evaluated in this study. Although it remains possible that certain combinations of SNPs in TAP1 and TAP2 could influence peptide transport by TAP and its resistance to viral inhibition, no consistent linkage disequilibrium has been found between TAP1 and TAP2 alleles (Alvarado-Guerri et al., 2005; Klitz et al., 1995).

Recent studies have revealed the mechanism that is used by the viral inhibitor ICP47 to block peptide transport by TAP (Blees et al., 2017; Luteijn and Wiertz, 2016; Oldham et al., 2016b). ICP47 affects peptide binding to TAP by trapping TAP in an inward-facing conformation (Oldham et al., 2016a). The molecular structure of TAP1-TAP2-ICP47 presented in these studies reveals that only the TAP1 SNPs S286F and A370V, and the TAP2 SNP A374T are located within potential interacting distance (8 Å) of ICP47 (Fig. 7). The most likely interaction would involve the TAP1 residue S286 that, when changed to phenylalanine, would create a more hydrophobic environment around the

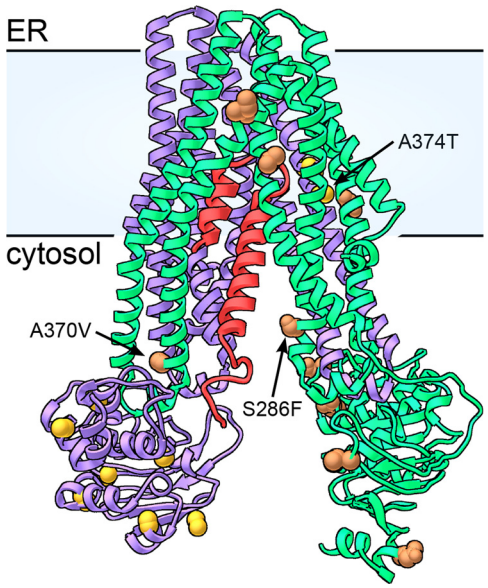

Fig. 7. Molecular model of the TAP1-TAP2-ICP47 complex. The viral inhibitor ICP47 (red) forms a helix-loop-helix structure and blocks TAP by obstructing the peptide translocation pathway with a helical hairpin. The SNPs S286F and A370V from TAP1 and A374T from TAP2 are located in close proximity to ICP47. (For interpretation of the references to colour in this figure legend, the reader is referred to the web version of this article.)

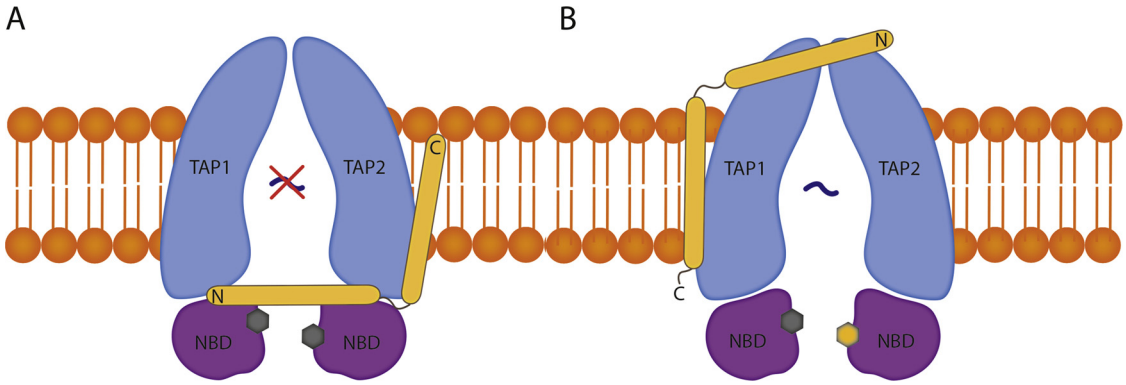

Fig. 8. Schematic representation of the interaction between the TAP complex and the viral inhibitors BNLF2a and US6. (A) Upon binding of the tail anchored transmembrane protein BNLF2a to TAP, peptide binding as well as ATP binding are inhibited. (B) In contrast to BNLF2a, the inhibitor US6 interferes with ATP binding to TAP1 while interacting with the ER-luminal loops of TAP1 and TAP2.

flexible C-terminal tail of ICP47. However, inhibition of TAP by ICP47 seems not to be influenced by any of the SNPs tested. The TAP1 SNPs V458L and I333V and the TAP2 SNP V379I are located in close proximity to the binding site of ICP47, yet do not directly interact with ICP47. Therefore, these SNPs are unlikely to affect the inhibitory capacity of ICP47.

In contrast to ICP47, HCMV US6 interacts with TM domains 7–10 of TAP1 and TM 1–4 of TAP2 to interfere with ATP binding to TAP1 (Halenius et al., 2005) (Fig. 8B). Since the exact binding site nor the structure of US6 and BNLF2a have been elucidated, assumptions about the specific mode of interaction of these inhibitors with TAP remain speculative. Furthermore, it is unknown if US6 and BNLF2a also arrest the TAP-complex in a stable conformation as does ICP47 (Herbring et al., 2016). It has been suggested that US6 interacts with the TAP1 and TAP2 TMDs and occupies the translocation pore from the luminal side (Halenius et al., 2005). Moreover, ICP47 and US6 cannot simultaneously bind to TAP (Matschulla et al., 2017). Therefore, it is likely that ICP47 and US6 bind to TAP at different stages during the peptide translocation cycle and thus target distinct conformations of TAP (reviewed in Praest et al., manuscript submitted).

A recent structural study has made clever use of ICP47 to isolate the fully assembled PLC (Blees et al., 2017). This study has provided crucial insights into the overall structure and stoichiometry of the PLC. However, the cytosolic part of the TAP heterodimer and the inhibitor ICP47 are resolved in a low resolution. Isolation of the PLC in the presence of US6 or BNLF2a will be instrumental to uncover the mechanisms by which these viral immune evasion proteins interfere with TAP function. Additionally, these studies may provide new insights into the structure of the PLC, in particular of those parts that remain to be resolved at high resolution.

Acknowledgements

We thank Dr. Jan Wouter Drijfhout from the Department of Immunohematology and Blood Transfusion at the Leiden University Medical Center, Leiden, The Netherlands, for generously providing reagents. This work was funded by the European Commission under the Horizon2020 program H2020 MSCA-ITN GA 675278 EDGE.

Appendix A. Supplementary data

Supplementary material related to this article can be found, in the online version, at doi:https://doi.org/10.1016/j.molimm.2018.05.025.

References

Ahn, K., Meyer, T.H., Uebel, S., Sempé, P., Djaballah, H., Yang, Y., Peterson, P.A., Früh, K., Tampé, R., 1996. Molecular mechanism and species specificity of TAP inhibition by herpes simplex virus ICP47. EMBO J. 15, 3247–3255.

Alvarado-Guerri, R., Cabrera, C.M., Garrido, F., López-Nevot, M.A., 2005. TAP1 and TAP2 polymorphisms and their linkage disequilibrium with HLA-DR, -DP, and -DQ in an eastern Andalusian population. Hum. Immunol. 66, 921–930. http://dx.doi.org/10.1016/j.humimm.2005.06.009.

Blees, A., Januliene, D., Hofmann, T., Koller, N., Schmidt, C., Trowitzsch, S., Moeller, A., Tampé, R., 2017. Structure of the human MHC-I peptide-loading complex. Nature 551, 525–528. http://dx.doi.org/10.1038/nature24627.

Borghans, J.A.M., Beltman, J.B., De Boer, R.J., 2004. MHC polymorphism under host-pathogen coevolution. Immunogenetics 55, 732–739. http://dx.doi.org/10.1007/s00251-003-0630-5.

Bullido, M.J., Martínez-García, A., Artiga, M.J., Aldudo, J., Sastre, I., Gil, P., Coria, F., Muñoz, D.G., Hachinski, V., Frank, A., Valdivieso, F., 2007. A TAP2 genotype associated with Alzheimer's disease in APOE4 carriers. Neurobiol. Aging 28, 519–523. http://dx.doi.org/10.1016/j.neurobiolaging.2006.02.011.

Carrillo-Bustamante, P., Keşmir, C., de Boer, R.J., 2015. A coevolutionary arms race between hosts and viruses drives polymorphism and polygenicity of NK cell receptors. Mol. Biol. Evol. 32, 2149–2160. http://dx.doi.org/10.1093/molbev/msv096.

Daniel, S., Caillat-Zucman, S., Hammer, J., Bach, J.F., van Endert, P.M., 1997. Absence of functional relevance of human transporter associated with antigen processing polymorphism for peptide selection. J. Immunol. 159, 2350–2357.

Dean, M., Annilo, T., 2005. Evolution of the Atp-binding cassette (ABC) transporter superfamily in vertebrates. Annu. Rev. Genomics Hum. Genet. 6, 123–142. http://dx.doi.org/10.1146/annurev.genom.6.080604.162122.

Fischbach, H., Döring, M., Nikles, D., Lehnert, E., Baldauf, C., Kalinke, U., Tampé, R., 2015. Ultrasensitive quantification of TAP-dependent antigen compartmentalization in scarce primary immune cell subsets. Nat. Commun. 6, 6199. http://dx.doi.org/10.1038/ncomms7199.

Gaudet, R., Wiley, D.C., 2001. Structure of the ABC ATPase domain of human TAP1, the transporter associated with antigen processing. EMBO J. 20, 4964–4972. http://dx.doi.org/10.1093/emboj/20.17.4964.

Halenius, A., Momburg, F., Reinhard, H., Bauer, D., Lobigs, M., Hengel, H., 2005. Physical and functional interactions of the cytomegalovirus US6 glycoprotein with the transporter associated with antigen processing. J. Biol. Chem. 281, 5383–5390. http://dx.doi.org/10.1074/jbc.M510223200.

Herbring, V., Bäucker, A., Trowitzsch, S., Tampé, R., 2016. A dual inhibition mechanism of herpesviral ICP47 arresting a conformationally thermostable TAP complex. Sci. Rep. 6, 36907. http://dx.doi.org/10.1038/srep36907.

Hewitt, E.W., Gupta, S.S., Lehner, P.J., 2001. The human cytomegalovirus gene product US6 inhibits ATP binding by TAP. EMBO J. 20, 387–396. http://dx.doi.org/10.1093/emboj/20.3.387.

Horst, D., van Leeuwen, D., Croft, N.P., Garstka, M.A., Hislop, A.D., Kremmer, E., Rickinson, A.B., Wiertz, E.J.H.J., Ressing, M.E., 2009. Specific targeting of the EBV lytic phase protein BNLF2a to the transporter associated with antigen processing results in impairment of HLA class I-restricted antigen presentation. J. Immunol. 182, 2313–2324. http://dx.doi.org/10.4049/jimmunol.0803218.

Keusekotten, K., Leonhardt, R.M., Ehses, S., Knittler, M.R., 2006. Biogenesis of functional antigenic peptide transporter TAP requires assembly of pre-existing TAP1 with newly synthesized TAP2. J. Biol. Chem. 281, 17545–17551. http://dx.doi.org/10.1074/jbc.M602360200.

Kim, H.K., Lee, H., Lew, B.L., Sim, W.Y., Kim, Y.O., Lee, S.W., Lee, S., Cho, I.K., Kwon, J.T., Kim, H.J., 2015. Association between TAP1 gene polymorphisms and alopecia areata in a Korean population. Genet. Mol. Res. 14, 18820–18827. http://dx.doi.org/10.4238/2015.December.28.31.

Klitz, W., Stephens, J.C., Grote, M., Carrington, M., 1995. Discordant patterns of linkage disequilibrium of the peptide-transporter loci within the HLA class II region. Am. J. Hum. Genet. 57, 1436–1444.

Koch, J., Guntrum, R., Heintke, S., Kyritsis, C., Tampe, R., 2004. Functional dissection of the transmembrane domains of the transporter associated with antigen processing (TAP). J. Biol. Chem. 279, 10142–10147. http://dx.doi.org/10.1074/jbc.M312816200.

Kubinak, J.L., Ruff, J.S., Cornwall, D.H., Middlebrook, E.A., Hasenkrug, K.J., Potts, W.K.,

2013. Experimental viral evolution reveals major histocompatibility complex polymorphisms as the primary host factors controlling pathogen adaptation and virulence. Genes Immun. 14, 365–372. http://dx.doi.org/10.1038/gene.2013.27.
Lajoie, J., Zijenah, L.S., Faucher, M.C., Ward, B.J., Roger, M., ZVITAMBO Study Group, 2003. Novel TAP1 polymorphisms in indigenous Zimbabweans: their potential implications on TAP function and in human diseases. Hum. Immunol. 64, 823–829.
Ljunggren, H.-G., Stam, N.J., Öhlén, C., Neefjes, J.J., Höglund, P., Heemels, M.-T., Bastin, J., Schumacher, T.N.M., Townsend, A., Kärre, K., Ploegh, H.L., 1990. Empty MHC class I molecules come out in the cold. Nature 346, 476–480. http://dx.doi.org/10.1038/346476a0.
Luteijn, R.D., Wiertz, E.J.H.J., 2016. Exploiting the exploiter: a viral inhibitor stabilizes TAP for cryo-EM. Nat. Struct. Mol. Biol. 23, 95–97. http://dx.doi.org/10.1038/nsmb.3168.
Matschulla, T., Berry, R., Gerke, C., Döring, M., Busch, J., Paijo, J., Kalinke, U., Momburg, F., Hengel, H., Halenius, A., 2017. A highly conserved sequence of the viral TAP inhibitor ICP47 is required for freezing of the peptide transport cycle. Sci. Rep. 7, 2933. http://dx.doi.org/10.1038/s41598-017-02994-5.
McCluskey, J., Rossjohn, J., Purcell, A.W., 2004. TAP genes and immunity. Curr. Opin. Immunol. 16, 651–659. http://dx.doi.org/10.1016/j.coi.2004.07.016.
Naderi, M., Hashemi, M., Aminiinia, S., 2016. Association of TAP1 and TAP2 Gene polymorphisms with susceptibility to pulmonary tuberculosis. Iran. J. Allergy Asthma Immunol. 15, 62–68.
Natter, C., Polterauer, S., Rahhal-Schupp, J., Cacsire Castillo-Tong, D., Pils, S., Speiser, P., Zeillinger, R., Heinze, G., Grimm, C., 2013. Association of TAP gene polymorphisms and risk of cervical intraepithelial neoplasia. Dis. Markers 35, 79–84. http://dx.doi.org/10.1155/2013/368732.
Neefjes, J.J., Momburg, F., Hämmerling, G.J., 1993. Selective and ATP-dependent translocation of peptides by the MHC-encoded transporter. Science 261, 769–771.
Nijenhuis, M., Hämmerling, G.J., 1996. Multiple regions of the transporter associated with antigen processing (TAP) contribute to its peptide binding site. J. Immunol. 157, 5467–5477.
Obst, R., Armandola, E.A., Nijenhuis, M., Momburg, F., Hämmerling, G.J., 1995. TAP polymorphism does not influence transport of peptide variants in mice and humans. Eur. J. Immunol. 25, 2170–2176. http://dx.doi.org/10.1002/eji.1830250808.
Oldham, M.L., Grigorieff, N., Chen, J., 2016a. Structure of the transporter associated with antigen processing trapped by herpes simplex virus. Elife 5. http://dx.doi.org/10.7554/eLife.21829.
Oldham, M.L., Hite, R.K., Steffen, A.M., Damko, E., Li, Z., Walz, T., Chen, J., 2016b. A mechanism of viral immune evasion revealed by cryo-EM analysis of the TAP transporter. Nature 529, 537–540. http://dx.doi.org/10.1038/nature16506.
Ozbas-Gerceker, F., Bozman, N., Gezici, S., Pehlivan, M., Yilmaz, M., Pehlivan, S., Oguzkan-Balci, S., 2013. Association of TAP1 and TAP2 gene polymorphisms with hematological malignancies. Asian Pac. J. Cancer Prev. 14, 5213–5217.
Parcej, D., Tampé, R., 2010. ABC proteins in antigen translocation and viral inhibition. Nat. Chem. Biol. 6, 572–580. http://dx.doi.org/10.1038/nchembio.410.
Pettersen, E.F., Goddard, T.D., Huang, C.C., Couch, G.S., Greenblatt, D.M., Meng, E.C., Ferrin, T.E., 2004. UCSF Chimera? A visualization system for exploratory research and analysis. J. Comput. Chem. 25, 1605–1612. http://dx.doi.org/10.1002/jcc.20084.
Plewnia, G., Schulze, K., Hunte, C., Tampé, R., Koch, J., 2007. Modulation of the antigenic peptide transporter TAP by recombinant antibodies binding to the last Five residues of TAP1. J. Mol. Biol. 369, 95–107. http://dx.doi.org/10.1016/j.jmb.2007.02.102.
Potts, W.K., Slev, P.R., 1995. Pathogen-based models favoring MHC genetic diversity. Immunol. Rev. 143, 181–197.
Powis, S.H., Tonks, S., Mockridge, I., Kelly, A.P., Bodmer, J.G., Trowsdale, J., 1993. Alleles and haplotypes of the MHC-encoded ABC transporters. Immunogenetics 37, 373–380.
Powis, S.J., Young, L.L., Joly, E., Barker, P.J., Richardson, L., Brandt, R.P., Melief, C.J., Howard, J.C., Butcher, G.W., 1996. The rat cim effect: TAP allele-dependent changes in a class I MHC anchor motif and evidence against C-terminal trimming of peptides in the ER. Immunity 4, 159–165.
Sadasivan, B., Lehner, P.J., Ortmann, B., Spies, T., Cresswell, P., 1996. Roles for calreticulin and a novel glycoprotein, tapasin, in the interaction of MHC class I molecules with TAP. Immunity 5, 103–114.
Tang, J., Freedman, D.O., Allen, S., Karita, E., Musonda, R., Braga, C., Jamieson, B.D., Louie, L., Kaslow, R.A., 2001a. Genotyping TAP2 variants in North American Caucasians, Brazilians, and Africans. Genes Immun. 2, 32–40. http://dx.doi.org/10.1038/sj.gene.6363731.
Tang, J., Freedman, D.O., Allen, S., Karita, E., Musonda, R., Braga, C., Margolick, J., Kaslow, R.A., 2001b. TAPI polymorphisms in several human ethnic groups: characteristics, evolution, and genotyping strategies. Hum. Immunol. 62, 256–268.
Townsend, A., Öhlén, C., Bastin, J., Ljunggren, H.-G., Foster, L., Kärre, K., 1989. Association of class I major histocompatibility heavy and light chains induced by viral peptides. Nature 340, 443–448. http://dx.doi.org/10.1038/340443a0.
van de Weijer, M.L., Bassik, M.C., Luteijn, R.D., Voorburg, C.M., Lohuis, M.A.M., Kremmer, E., Hoeben, R.C., LeProust, E.M., Chen, S., Hoelen, H., Ressing, M.E., Patena, W., Weissman, J.S., McManus, M.T., Wiertz, E.J.H.J., Lebbink, R.J., 2014. A high-coverage shRNA screen identifies TMEM129 as an E3 ligase involved in ER-associated protein degradation. Nat. Commun. 5, 3832. http://dx.doi.org/10.1038/ncomms4832.
van de Weijer, M.L., Luteijn, R.D., Wiertz, E.J.H.J., 2015. Viral immune evasion: lessons in MHC class I antigen presentation. Semin. Immunol. 27, 125–137. http://dx.doi.org/10.1016/j.smim.2015.03.010.
van Diemen, F.R., Kruse, E.M., Hooykaas, M.J.G., Bruggeling, C.E., Schürch, A.C., van Ham, P.M., Imhof, S.M., Nijhuis, M., Wiertz, E.J.H.J., Lebbink, R.J., 2016. CRISPR/Cas9-mediated genome editing of herpesviruses limits productive and latent infections. PLoS Pathog. 12, e1005701. http://dx.doi.org/10.1371/journal.ppat.1005701.
van Endert, P.M., Tampé, R., Meyer, T.H., Tisch, R., Bach, J.F., McDevitt, H.O., 1994. A sequential model for peptide binding and transport by the transporters associated with antigen processing. Immunity 1, 491–500.
Verweij, M.C., Horst, D., Griffin, B.D., Luteijn, R.D., Davison, A.J., Ressing, M.E., Wiertz, E.J.H.J., 2015. Viral inhibition of the transporter associated with antigen processing (TAP): a striking example of functional convergent evolution. PLoS Pathog. 11, e1004743. http://dx.doi.org/10.1371/journal.ppat.1004743.
Walker, J.E., Saraste, M., Runswick, M.J., Gay, N.J., 1982. Distantly related sequences in the alpha- and beta-subunits of ATP synthase, myosin, kinases and other ATP-requiring enzymes and a common nucleotide binding fold. EMBO J. 1, 945–951.
Wang, D., Zhou, Y., Ji, L., He, T., Lin, F., Lin, R., Lin, T., Mo, Y., 2012. Association of LMP/TAP gene polymorphisms with tuberculosis susceptibility in Li population in China. PLoS One 7, e33051. http://dx.doi.org/10.1371/journal.pone.0033051.
Webb, B., Sali, A., Webb, B., Sali, A., 2014. Comparative protein structure modeling using MODELLER. Current Protocols in Bioinformatics. John Wiley & Sons, Inc., Hoboken, NJ, USA. http://dx.doi.org/10.1002/0471250953.bi0506s47. 5.6.1–5.6.32.